# Selective adsorption and electronic interaction of $F_{16}CuPc$ on epitaxial graphene

Yi-Lin Wang,[1,2] Jun Ren,[3] Can-Li Song,[1,2] Ye-Ping Jiang,[2,1] Li-Li Wang,[1] Ke He,[1] Xi Chen,[2] Jin-Feng Jia,[2] Sheng Meng,[1,3,*,†] Efthimios Kaxiras,[3] Qi-Kun Xue,[2,1] and Xu-Cun Ma[1,*,‡]

[1]*Institute of Physics, Chinese Academy of Sciences, Beijing 100190, China*

[2]*Department of Physics, Tsinghua University, Beijing 100084, China*

[3]*Insitute of Materials, École Polytechnique Fédérale de Lausanne (EPFL), CH-1015 Lausanne, Switzerland*

(Received 17 November 2010; published 14 December 2010)

We investigate the electronic coupling between copper hexadecafluoro-phthalocyanine ($F_{16}CuPc$) and epitaxial graphene (EG) on 6H-SiC(0001) using a combined approach of low-temperature scanning tunneling spectroscopy and electronic structure calculations. The molecules are preferentially adsorbed on monolayer EG than bilayer EG. Competing molecule-surface and intermolecular van der Waals interactions result in two well-ordered incommensurate phases. We show that the amount of charge transfer from EG to $F_{16}CuPc$ can be tuned by applied voltage or the thickness of graphene layers. A characteristic feature at ~0.4 eV above the Dirac point is identified in bilayer EG, which indicates its electronic structure is modified via introducing extra unoccupied states upon adsorption.

DOI: 10.1103/PhysRevB.82.245420 PACS number(s): 73.22.Pr, 68.43.−h, 68.37.Ef, 31.15.E−

Graphene, a single layer of carbon atoms arranged in a honeycomb lattice, has attracted great attention due to remarkable physical properties and potential for different electronic devices since its discovery[1,2] in 2004. To develop graphene-based electronics, one of the most critical issues is the precise control of carriers in graphene layer. Thermal decomposition of silicon carbide (SiC) yields wafer-size graphene supported on a semi-insulating substrate, making it one of the most promising methods for mass production of graphene.[3,4] In this case, modulation of carriers in graphene can be achieved either by applying an external gate voltage[1,5] or by chemical doping.[6–14] Upon adsorption of metal atoms[8,14] or molecules,[6,7,9–13] electrons or holes are introduced to graphene via charge transfer. The adsorbates can also act as charged impurities and scattering centers, which alter the transport properties such as carrier mobility.[5] Precise carrier control in graphene requires a comprehensive understanding of the interfacial structure and interaction between adsorbates and graphene.

Here we employ a combined scanning tunneling microscopy/spectroscopy (STM/STS) and theoretical approach to study the adsorption behavior of copper hexadecafluoro-phthalocyanine ($F_{16}CuPc$) on both monolayer and bilayer epitaxial graphene (EG) layers formed on SiC(0001). Specifically, we pay attention to modification of the electronic structure of graphene by the molecule. $F_{16}CuPc$ was chosen because it is a representative $\pi$-conjugated molecule and strong electron acceptor, which has widely been used in *n*-type organic semiconductor devices. STM/STS provide both high spatial and spectroscopic resolution and have recently been used to reveal the novel features in graphene layers on SiC.[15–17] By combining STM/STS experiments and first-principles calculations, we are able to identify a unique modification on electronic structure of graphene upon $F_{16}CuPc$ adsorption. In addition, we show that by varying the thickness of the graphene layers or the applied voltage, we can tune the adsorption and the amount of charge transfer to the molecule, which constitutes a novel approach to interfacial structure engineering and carrier control, in essence achieving controlled doping without chemical substitution.

The experiments were performed in a Unisoku ultrahigh vacuum low-temperature-STM system, which is equipped with a molecular-beam epitaxy chamber for *in-situ* sample preparation. EG was prepared on nitrogen doped 6H-SiC(0001) substrate using solid-state graphitization.[6] Coexisting monolayer EG (MEG) and bilayer EG (BEG) surfaces were formed at the graphitization temperature $T=1300$ °C, on which $F_{16}CuPc$ molecules were deposited. $F_{16}CuPc$ molecules [Sigma-Aldrich, the schematic molecular structure is shown in the inset of Fig. 1(a)] were evaporated from a Knudsen cell onto EG at room temperature. The deposition flux rate was ~0.01 ML/min. Here, 1 ML is defined as the surface coverage of the most close-packed $F_{16}CuPc$ mono-

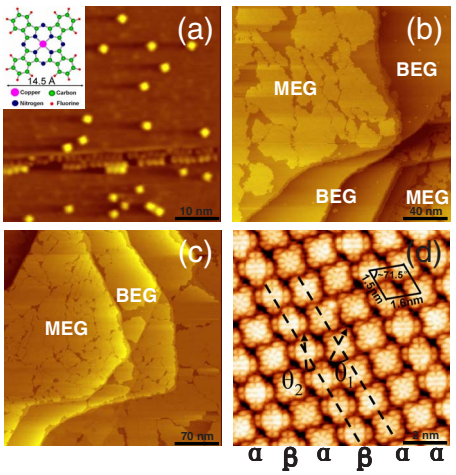


FIG. 1. (Color online) [(a)–(c)] STM images showing $F_{16}CuPc$ adsorption at different coverage on the EG surface. (a) 0.1 ML ($50\times50$ nm$^2$, $V=2.3$ V, $I=0.1$ nA). (b) 0.4 ML ($200\times200$ nm$^2$, $V=5.0$ V, $I=0.1$ nA). (c) 0.9 ML ($350\times350$ nm$^2$, $V=5.0$ V, $I=0.1$ nA). Selective adsorption on MEG is clearly seen in (b). The inset shows the structure of $F_{16}CuPc$ molecule. (d) High-resolution image of $F_{16}CuPc$ on EG ($10\times10$ nm$^2$, $V=1.5$ V, $I=0.1$ nA), where the dashed lines indicate orientations of molecular rows and arrows indicate molecular axes.

 

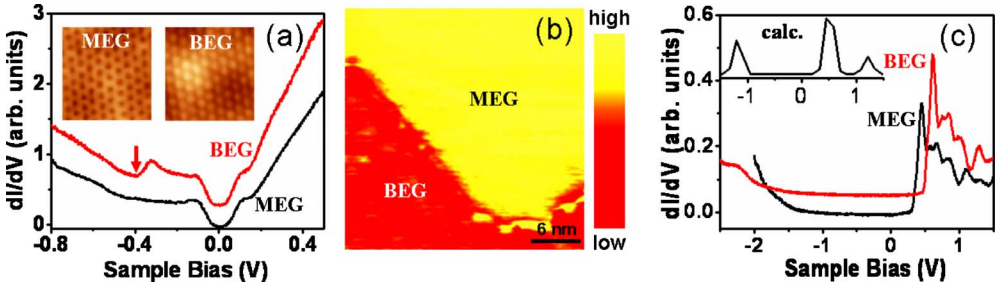


FIG. 2. (Color online) (a) Representative $dI/dV$ curves on MEG (lower) and BEG (upper), the arrow marks the Dirac point of BEG. The tunneling junction is set at $V=0.3$ V and $I=0.1$ nA. The curves are vertically shifted for clarity. The insets show atomic-resolution images ($2\times2$ nm$^2$) of MEG and BEG, respectively. (b) LDOS map of the EG surface at $V=0.03$ V. (c) STS spectra performed on $F_{16}$CuPc molecules adsorbed on MEG (lower) and BEG (upper), respectively. The tunneling junction is set at $V=1.0$ V and $I=0.1$ nA. The inset is the calculated LDOS on $F_{16}$CuPc. Spectra are vertically displaced for clarity.

layer ($10^{13}$ molecules/cm$^2$). STM measurement was performed at 4.8 K in the constant current mode using electrochemically etched polycrystalline W tips. The STS spectra were acquired using standard lock-in technique with a bias modulation of 20 mV (r.m.s.) at 987.5 HZ.

The first-principles calculations were performed within the framework of density functional theory (DFT) as implemented in the SIESTA CODE.[18] We use pseudopotentials of the Troullier-Martins type, the local-density approximation and hybrid Heyd-Scuseria-Ernzerhof (HSE) functional for exchange-correlation energy, and a local basis set of double $\zeta$ polarized orbitals (13 orbitals for C, N, F, and O). An auxiliary real-space grid equivalent to a plane-wave cutoff of 120 Ry and $k$-point mesh of $(8\times8\times1)$ in Monkhorst-Pack sampling is employed and spin polarization is included whenever necessary. Basis-set superposition errors are excluded in relative energies. The atomic structure is considered fully relaxed when the magnitude of forces on every atom is smaller than 0.04 eV/Å.

Figure 1 shows the adsorption behavior of $F_{16}$CuPc on EG from submonolayer to full coverage. Preferential nucleation at lower step edges is clearly noted [Fig. 1(a)], indicating a van der Waals-type $F_{16}$CuPc-EG interaction and appreciable diffusion of the molecules at room temperature. Upon completion of step edges by $F_{16}$CuPc, random nucleation and growth of two-dimensional (2D) islands on terrace are observed when the coverage increases to 0.4 ML, as shown in Fig. 1(b). The random nucleation eventually leads to a multidomain self-assembled monolayer at 0.9 ML [see Fig. 1(c)]. In the high-resolution STM image [Fig. 1(d)], which is zoomed in from the self-assembled monolayer, each molecule is imaged as a four-lobe structure, which is in agreement with its molecular structure in Fig. 1(a). The observation indicates that the $F_{16}$CuPc molecule adopts a flat configuration with the $\pi$-plane parallel to the surface. The close-packing direction is aligned roughly with the C-C bond directions of the graphene substrate. The adsorbed molecules take primarily two orientations, denoted as $\alpha$ and $\beta$ orientation, respectively [Fig. 1(d)]. The ordering of differently oriented molecules leads to two distinct molecular rows [see the dashed lines in Fig. 1(d)], and the self-assembled monolayer is thus composed of alternatively arranged $\alpha$ and $\beta$ rows (called as $\alpha\beta$ phase hereafter). Similar structure was observed for $F_{16}$CuPc on highly oriented pyrolytic graphite.[19] A major difference is that in the latter case, more molecules have the same $\alpha$ orientation (called as $\alpha\alpha$ phase hereafter). As a result, the resulted molecular density is higher (0.946 molecules/nm$^2$) compared to the present case (0.874 molecules/nm$^2$). The lower density in this study implies a larger amount of charge transfer occurring between molecules and the surface.

In spite of the weak interaction between $F_{16}$CuPc and EG, the formation of multidomain monolayer implies that the diffusion is limited. Our first-principles calculations show that the diffusion barrier of $F_{16}$CuPc on MEG is ~0.2 eV. More interestingly, there is an evidenced selective adsorption behavior. As shown in Fig. 1(b), ordered molecular islands are formed and randomly dispersed over certain terraces, while the other terraces are completely free of molecules. The STM images obtained from areas beneath molecular islands (molecules can be removed by scanning at low bias) show strong features of MEG while bare terraces without molecule adsorption can be identified as BEG. When the surface of MEG is fully covered by increasing the coverage, the molecules eventually start to occupy the BEG surface as well. Clearly, this is not a kinetics-limited phenomenon. As discussed below, the selective adsorption arises from a subtle difference in the electronic structures of MEG and BEG.

In STS, the $dI/dV$ spectrum measures the local electronic density of states (LDOS). In Fig. 2(a), we show the $dI/dV$ curves of both MEG and BEG, together with their high-resolution STM images [see the insert]. The $dI/dV$ curves were obtained by averaging the spectra over more than fifty locations. The carbon-rich buffer layer with a $(6\times6)$ superstructure shows up in both STM images, and MEG exhibits a rougher surface.[17] The ~130 meV gap centered at 0 V (the Fermi energy, $E_F$),[16] which originates from the phonon-mediated inelastic tunneling process and agrees with the previous study,[20] indicates MEG is supported on the buffer layer via weak van der Waals forces. The Dirac point [$E_D$, indicated by the arrow in Fig. 2(a)] of BEG is located at $390\pm15$ meV below $E_F$. Due to the contribution of the buffer layer to the tunneling current, the $E_D$ of MEG is nearly invisible with a small dip at −550 meV. According to previous Angle-resolved Photoemission Spectroscopy (ARPES) results that the $E_D$ of MEG is 140 meV lower than that of BEG,[21] the $E_D$ of MEG is estimated to be ~550 meV below $E_F$. These values are more consistent with ARPES

measurements (−300 meV and −440 meV for BEG and MEG, respectively[21]) if the photon energy of 67 meV in inelastic tunneling processes is removed from STS values.[20] However, the precise location of $E_D$ is not a focus of this paper and does not alter our main findings. The shifting toward the Fermi energy with increasing thickness is also consistent with other experiments.[17,21,22] We then carried out $dI/dV$ mapping,[23] which measures the total LDOS. The result is shown in Fig. 2(b), from which we can clearly see that the LDOS of MEG is higher than that of BEG. The LDOS difference between MEG and BEG arises from the different amount of charge transfer. The EG/SiC is *n*-type doped due to charge transfer from the interface.[21] Because of the small interlayer screening length ($<1.4$ Å), the charge densities in top layer of BEG is much smaller than that of MEG.

Similar adsorption behavior has been observed when depositing CoPc molecules on Pb film surfaces. Adsorption sequence has one-to-one correspondence to the quantum-size-effect modulated LDOS near $E_F$ (details in Ref. 23). The $F_{16}$CuPc molecule studied here is similar to CoPc in the structure and properties, implying the selective adsorption can occur on both Pb and graphene surfaces. We found again that higher LDOS near $E_F$ corresponds to earlier adsorption sequence. Our first-principles calculations show that the adsorption energy of $F_{16}$CuPc on MEG and BEG is 2.3 eV and 2.0 eV, respectively. The energy difference (0.3 eV), together with the small diffusion barrier (0.2 eV), can well explain the observed selective adsorption as shown in Fig. 1.

To understand the ordered structures, we carried out modeling of the adsorption system with first-principles DFT calculations. Supercells containing one (for the $\alpha\alpha$ phase) or two (for the $\alpha\beta$ phase) $F_{16}$CuPc molecules on isolated graphene are used with periodic boundary conditions. We considered both neutral and charged systems; the latter is invoked to model the interfacial charge transfer from the SiC substrate. For MEG and BEG, $E_F$ is approximately 0.6 eV and 0.4 eV above $E_D$, respectively. From our first-principles calculations, this corresponds to a total charge of $0.01e$ and $0.005e$ per carbon atom. According to the unit-cell size ($15.0\times16.0$ Å$^2$ with a vector angle of 71.5°) in Fig. 1(d), an incommensurate overlayer (or a commensurate layer with a very large unit cell) forms on the graphene. The modeling reveals that the best matching supercell is $(4,3)\times(3,4)$, and the corresponding unit-cell size is 14.961 Å with a vector angle of 69.4°. In the following, we use this model for the $\alpha\alpha$ phase while $(4,3)\times(6,8)$ for the $\alpha\beta$ phase.

Our calculations show that two phases have nearly identical formation energies, and that the $\alpha\alpha$ phase is only slightly favored by 0.1 eV per molecule. However, the intermolecular interaction differs significantly: it is attractive (−0.27 eV) in the $\alpha\alpha$ phase but repulsive (+0.23 eV) in the $\alpha\beta$ phase in the chosen unit cell. To reflect the real dimension in experiment [Fig. 1(d)], we expanded one of the cell vectors of the molecular layer by itself by 1 Å; this is a useful approach in dealing with interactions within a layer which is incommensurate with the substrate, as shown in Ref. 24. With this change the intermolecular interaction in both $\alpha\alpha$ and $\alpha\beta$ phases becomes attractive (∼0.5–0.7 eV). More importantly, the $\alpha\beta$ phase is found to be more energetically favored by 0.22 eV than the $\alpha\alpha$ phase, in agreement with experiment. Our calculations for a smaller or larger expansion of the molecular layer cell vector give the same trend. Therefore, it is a delicate balance between $F_{16}$CuPc-EG interaction and the intermolecular attraction that gives rise to the observed $\alpha\beta$ phase.

The STS of $F_{16}$CuPc molecules adsorbed on MEG and BEG, shown in Fig. 2(c), provide valuable insight to the electronic interaction between the molecule and EG. The lowest unoccupied molecular orbitals (LUMOs) of $F_{16}$CuPc exhibit distinct features on both MEG and BEG. For example, on MEG, in addition to the sharp peak at 0.44 eV three to four resonancelike peaks evenly separated by ∼0.2 eV show up at higher energies, which will be discussed later. Another significant feature in Fig. 2(c) is that the LUMOs of $F_{16}$CuPc on MEG shift by 0.17 eV toward $E_F$ compared to that on BEG, implying that the charge transfer occurs between $F_{16}$CuPc and EG. Our DFT calculations indicate that the LUMOs of $F_{16}$CuPc remains constant with respect to $E_D$ for both MEG and BEG. However, the $E_F$ is shifted by 0.2 eV toward $E_D$ from MEG to BEG, which can account for the upshift of 0.17 eV of LUMOs with respect to $E_F$ in BEG [Fig. 2(c)].

Figure 3 displays the calculated electron densities. From corresponding DOS plots we find that the HOMOs and LUMOs are located at ∼1.2 eV below and ∼0.4 eV above $E_F$, respectively, yielding an energy gap of ∼1.6 eV [Fig. 2(c)]. We find that for neutral systems the $E_F$ is 40 meV below the $E_D$ of graphene and the LUMOs of $F_{16}$CuPc are partially occupied, indicating a charge-transfer effect. From electron-density differences induced by $F_{16}$CuPc adsorption in Figs. 3(a)–3(c), it is clear that the $p_z$ orbitals of both graphene and the molecule are mainly involved in the strong $\pi\pi$ interaction. Integrating the charge-density difference along the surface normal to the graphene plane shows a net charge transfer of approximately $0.1e$ from graphene to molecule [Fig. 3(d)], which is mainly distributed around the central Cu atom and the F-substitutional phenyl rings on the perimeter of the molecule. It leads to an electron depletion in $p_z$ orbitals and a charge accumulation in $\sigma^*$ orbitals of the base plane of graphene (especially beneath the phenyl rings). When the system is negatively charged by $0.4e$ ($0.8e$) to reflect the effect of SiC substrate on BEG (MEG), the net charge transfer will increase to $0.32e$ ($0.57e$) by the same analysis [Fig. 3(e)]. In contrast, the positively charged graphene by $0.4e$ will introduce opposite electron transfer of $0.06e$ from $F_{16}$CuPc to graphene [Fig. 3(e)]. This provides a convenient way to control molecule-graphene charge transfer by applying bias on graphene (charging effect) or even by simply changing the thickness of EG. Thus, we have demonstrated not only selective molecular adsorption on graphene, but also that electronic couplings can be tailored through this approach, which is of critical importance for surface patterning, carrier control, and nanoelectronics. The resulting STM images simulated from DFT (Fig. 3) are in great agreement with the experiment [Fig. 1(d)]. Hence, the $\pi$-orbital hybridization and charge-transfer account for the main character of the $F_{16}$CuPc-graphene interaction.

Our calculations reveal that the $F_{16}$CuPc LUMOs have four degenerate molecular orbitals (two spin-up and two spin-down), and a spin-down orbital which is 0.7 eV higher

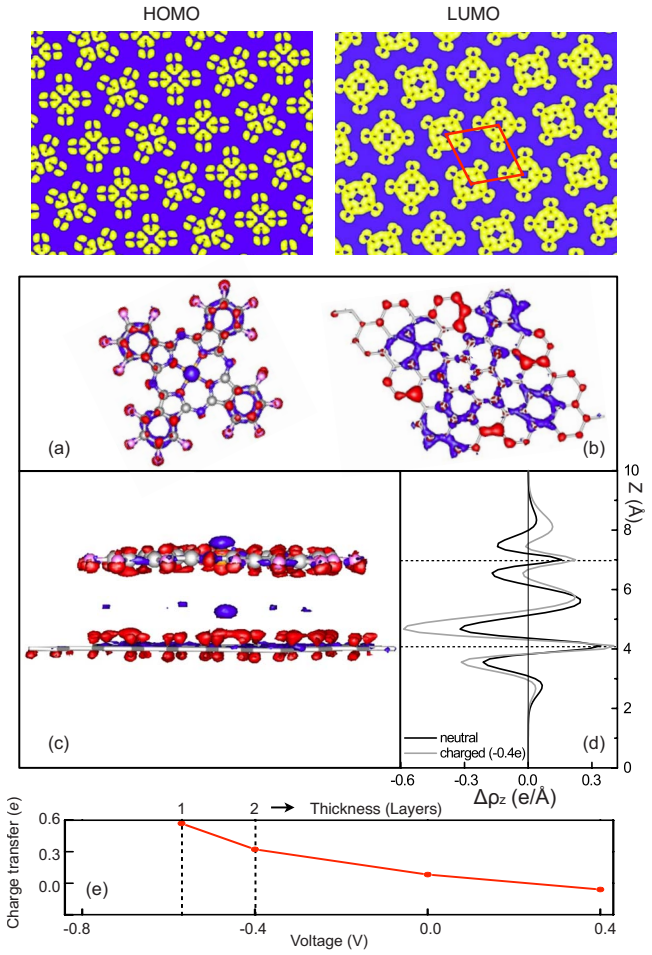


FIG. 3. (Color online) Upper panels: simulated STM images for the occupied HOMO states (left) and the unoccupied LUMO states (right). Lower panels: [(a) and (b)] top view and (c) side view of the charge-density difference upon $F_{16}CuPc$ adsorption on graphene at contour levels of $\pm 0.003$ $e/Å^3$. The blue/black and red/gray clouds correspond to regions with electron accumulation and depletion, respectively. (d) The plane-averaged charge-density difference along the surface-normal direction of graphene for the neutral system (black line) and a system charged by $-0.4e$ (gray line). Horizontal dashed lines indicate the position of graphene layer and $F_{16}CuPc$. (e) The amount of electron transfer from graphene to $F_{16}CuPc$ as a function of applied bias V on graphene. Cases at $V=0.39$ V and 0.55 V correspond to BEG ($n=2$) and MEG ($n=1$), respectively, where $n$ is the number of graphene layers on SiC.

in energy [Fig. 2(c)]. The latter may correspond to the peak at 1.09 eV in STS. As for the multipeak STS spectra, we can first rule out the following possibilities: (i) $F_{16}CuPc$ anions, which have charges $\geq -1$, do not give rise to a similar pattern in LUMO energies. (ii) 2D free electron proposed in Ref. 25 is not applicable since the energy splitting will be smaller than 30 meV for a molecular island with diameters of $>20$ nm. (iii) From band-structure calculations, dispersion of the flat LUMO bands is $<0.1$ eV even the $F_{16}CuPc$ lattice is compressed/expanded by as much as 10%. The lattice compression/expansion cannot account for the STS data. (iv) Different molecular orientations can also give rise to a splitting. But it is usually smaller than 0.1 eV. We therefore

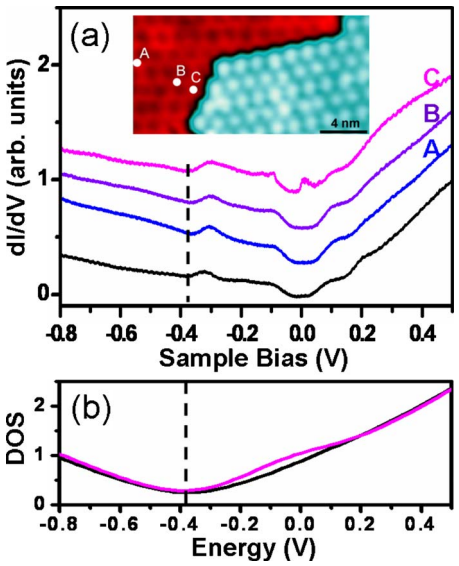


FIG. 4. (Color online) (a) STS spectra obtained on clean BEG (black line) and on the points (A–C) approaching the molecular island boundary. The corresponding STM image is shown in the inset ($20\times 10$ nm$^2$, $V=2.2$ V, $I=0.1$ nA). All spectra are obtained at the tunneling junctions at $V=0.3$ V and $I=0.1$ nA. The spectra are offset vertically for clarity. (b) Calculated DOS for isolated graphene (black curve) and for graphene in the $F_{16}CuPc$/graphene system (pink/gray curve). Theoretical curves have been shifted by aligning the Dirac point ($E_D$, dashed line) to that measured by STS.

speculate that the additional features in STS come from local molecular vibrations excited by the tunneling current, particularly the C-N-C stretching, which has an energy of 0.191 eV.[26] Vibrational excitations at $\sim 61-104$ meV were indeed observed in the STS measurement of similar molecule—CuPc on $Al_2O_3$/NiAl (110).[27]

Our study also reveals a prominent modification of the electronic states of EG by $F_{16}CuPc$ molecule. The series of $dI/dV$ curves shown in Fig. 4(a) were obtained at three different locations (A, B, and C) on BEG near an $F_{16}CuPc$ island [see the insert STM image]. For comparison, the $dI/dV$ spectra (the black curve) of the bare BEG is also shown. The $E_D$ of BEG does not show any noticeable change [see the dashed line]. It is not surprising because the electron depletion region in graphene is centered around the molecule and the charge transfer is small ($0.3e$). Due to screening effect, the charge-density change near the molecule is too small to induce obvious shift in $E_D$. A new observation is the peak near the $E_F$ at the location very close to the island edge (curve C). To understand the origin of this peak, we compare the DOS of bare graphene with that of the present system in Fig. 4(b). The DOS of graphene is greatly changed upon $F_{16}CuPc$ adsorption: the major peak at 2.3 eV below $E_D$ is significantly reduced and more states show up at 1.8 eV below $E_D$ (not shown). In addition, a small feature shows up at $\sim 0.4$ eV above $E_D$, which agrees well with the new peak in Fig. 4(a). This result indicates that the electronic states of graphene are modified upon $F_{16}CuPc$ adsorption, which destabilizes $p_z$ bonding states and introduces extra unoccupied states, consistent with the charge-density analysis in Fig. 3(b). According to Fig. 4(a), the charge depleted area in BEG

is in a range from 1 to 2 nm, and the charge is delocalized to some extent. Therefore, homogeneous doping of graphene can indeed be achieved by appropriate molecular adsorption.

In conclusion, we have demonstrated the adsorption behavior of $F_{16}$CuPc on EG/SiC(0001) and its influence on the electronic structure of EG. By varying the layer thickness, selective adsorption on MEG is achieved and analyzed in terms of electronic effects, specifically the LDOS ($E_F$). Through these features, the interface charge transfer can be engineered in a controllable fashion. We show that the electronic states of graphene are modified via introducing extra unoccupied states and tunable electron couplings.

This work was financially supported by the National Natural Science Foundation and the Ministry of Science and Technology of China. S.M. acknowledges financial support from the hundred-talent program of CAS.

*Corresponding author.
†smeng@iphy.ac.cn
‡xcma@aphy.iphy.ac.cn

[1] K. S. Novoselov, A. K. Geim, S. V. Morozov, D. Jiang, Y. Zhang, S. V. Dubonos, I. V. Grigorieva, and A. A. Firsov, Science **306**, 666 (2004).
[2] A. K. Geim and K. S. Novoselov, Nature Mater. **6**, 183 (2007).
[3] C. Berger, Z. M. Song, T. B. Li, X. B. Li, A. Y. Ogbazghi, R. Feng, Z. T. Dai, A. N. Marchenkov, E. H. Conrad, P. N. First, and W. A. de Heer, J. Phys. Chem. B **108**, 19912 (2004).
[4] K. V. Emtsev, A. Bostwick, K. Horn, J. Jobst, G. L. Kellogg, L. Ley, J. L. McChesney, T. Ohta, S. A. Reshanov, J. Rohrl, E. Rotenberg, A. K. Schmid, D. Waldmann, H. B. Weber, and T. Seyller, Nature Mater. **8**, 203 (2009).
[5] J. H. Chen, C. Jang, S. Adam, M. S. Fuhrer, E. D. Williams, and M. Ishigami, Nat. Phys. **4**, 377 (2008).
[6] W. Chen, S. Chen, D. C. Qi, X. Y. Gao, and A. T. S. Wee, J. Am. Chem. Soc. **129**, 10418 (2007).
[7] J. T. Sun, Y. H. Lu, W. Chen, Y. P. Feng, and A. T. S. Wee, Phys. Rev. B **81**, 155403 (2010).
[8] I. Gierz, C. Riedl, U. Starke, C. R. Ast, and K. Kern, Nano Lett. **8**, 4603 (2008).
[9] T. O. Wehling, K. S. Novoselov, S. V. Morozov, E. E. Vdovin, M. I. Katsnelson, A. K. Geim, and A. I. Lichtenstein, Nano Lett. **8**, 173 (2008).
[10] P. Lauffer, K. V. Emtsev, R. Graupner, T. Seyller, and L. Ley, Phys. Status Solidi B **245**, 2064 (2008).
[11] Y. H. Lu, W. Chen, Y. P. Feng, and P. M. He, J. Phys. Chem. B **113**, 2 (2009).
[12] C. Coletti, C. Riedl, D. S. Lee, B. Krauss, L. Patthey, K. von Klitzing, J. H. Smet, and U. Starke, Phys. Rev. B **81**, 235401 (2010).
[13] A. K. Manna and S. K. Pati, Chem. Asian J. **4**, 855 (2009).
[14] T. Ohta, A. Bostwick, T. Seyller, K. Horn, and E. Rotenberg, Science **313**, 951 (2006).
[15] G. M. Rutter, J. N. Crain, N. P. Guisinger, T. Li, P. N. First, and J. A. Stroscio, Science **317**, 219 (2007).
[16] V. W. Brar, Y. Zhang, Y. Yayon, T. Ohta, J. L. McChesney, A. Bostwick, E. Rotenberg, K. Horn, and M. F. Crommie, Appl. Phys. Lett. **91**, 122102 (2007).
[17] P. Lauffer, K. V. Emtsev, R. Graupner, T. Seyller, L. Ley, S. A. Reshanov, and H. B. Weber, Phys. Rev. B **77**, 155426 (2008).
[18] J. M. Soler, E. Artacho, J. D. Gale, A. Garcia, J. Junquera, P. Ordejón, and D. Sánchez-Portal, J. Phys.: Condens. Matter **14**, 2745 (2002).
[19] Y. L. Huang, W. Chen, S. Chen, and A. T. S. Wee, Appl. Phys. A: Mater. Sci. Process. **95**, 107 (2009).
[20] Y. Zhang, V. W. Brar, F. Wang, C. Girit, Y. Yayon, M. Panlasigui, A. Zettl, and M. F. Crommie, Nat. Phys. **4**, 627 (2008).
[21] T. Ohta, A. Bostwick, J. L. McChesney, T. Seyller, K. Horn, and E. Rotenberg, Phys. Rev. Lett. **98**, 206802 (2007).
[22] S. Y. Zhou, G. H. Gweon, A. V. Fedorov, P. N. First, W. A. De Heer, D. H. Lee, F. Guinea, A. H. C. Neto, and A. Lanzara, Nature Mater. **6**, 770 (2007).
[23] P. Jiang, X. C. Ma, Y. X. Ning, C. L. Song, X. Chen, J. F. Jia, and Q. K. Xue, J. Am. Chem. Soc. **130**, 7790 (2008).
[24] S. Y. Quek, M. M. Biener, J. Biener, J. Bhattacharjee, C. M. Friend, U. V. Waghmare, and E. Kaxiras, J. Chem. Phys. **127**, 104704 (2007).
[25] R. Temirov, S. Soubatch, A. Luican, and F. S. Tautz, Nature (London) **444**, 350 (2006).
[26] F. C. Wu, H. L. Cheng, C. H. Yen, J. W. Lin, S. J. Liu, W. Y. Chou, and F. C. Tang, Phys. Chem. Chem. Phys. **12**, 2098 (2010).
[27] X. H. Qiu, G. V. Nazin, and W. Ho, Phys. Rev. Lett. **92**, 206102 (2004).